RADC-TR-71-292
Technical Report
September 1971

Prepared By
Rome Air Development Center
Air Force Systems Command
Griffiss Air Force Base, New York 13440

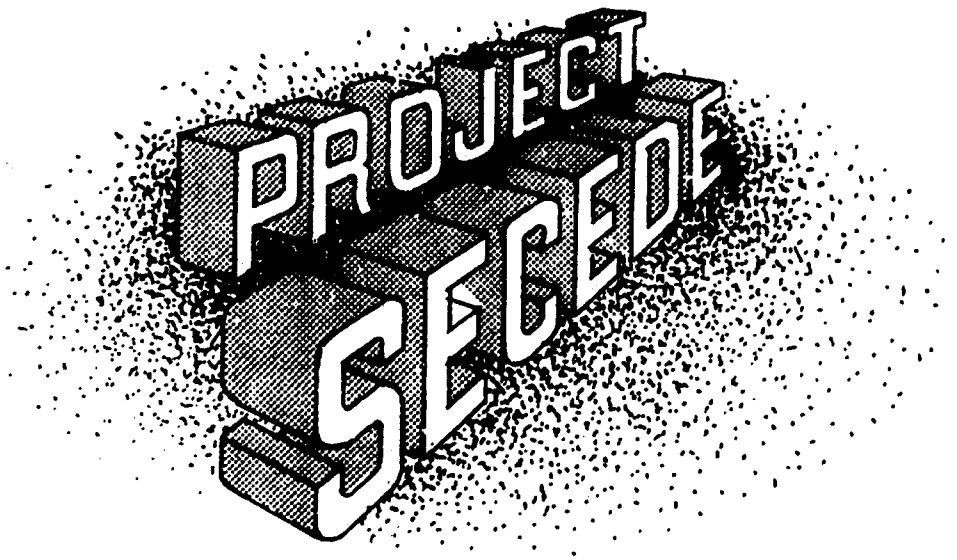

POLARIZATION, STEEPENING AND STRIATION IN BARIUM CLOUDS

University of Rochester

Sponsored by
Advanced Research Projects Agency
ARPA Order No. 1057

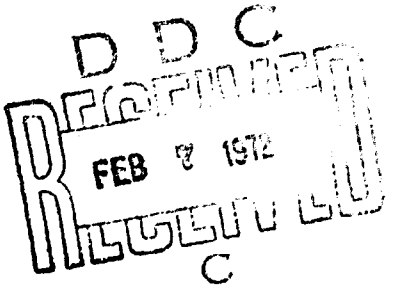

POLARIZATION, STEEPENING AND STRIATION IN BARIUM CLOUDS

Albert Simon
Arthur M. Sleeper

Contractor: University of Rochester
Contract Number: F30602-70-C-0001
Effective Date of Contract: 14 September 1969
Contract Expiration Date: 14 September 1971
Amount of Contract: $65,063.00
Program Code Number: 1E20

Principal Investigator: Professor Albert Simon
Phone: 716 275-4071

Project Engineer: Vincent J. Coyne
Phone: 315 330-3107

Contract Engineer: Leonard Strauss
Phone: 315 330-4907

This research was supported by the
Advanced Research Projects Agency
of the Department of Defense and
was monitored by Leonard Strauss
RADC (OCSE), GAFB, NY 13440 under
contract F30602-70-C-0001.

PUBLICATION REVIEW

This technical report has been reviewed and is approved.

Joseph J. Simna for

VINCENT J. COYNE
RADC Project Engineer

Leonard Strauss

LEONARD STRAUSS
RADC Contract Engineer

ABSTRACT

Numerical results are presented for the diffusive growth in time of a barium cloud in a highly (but not infinitely) conducting ionosphere. Polarization effects produce steepening of the backside and a thinning and indentation on the front side. A crude estimate of the time required for appreciable distortion is given.

Numerical results are also given for the linearized equations of motion about an ellipsoidal gaussian equilibrium distribution. A new numerical method yields the fastest growing eigenvalue and eigenfunction and has been pushed to 49 x 49 size grids covering the cloud. The resultant eigenfunctions (in the plane perpendicular to the B field) are concentrated in the rear of the cloud and are elongated parallel to the cloud drift velocity. Finally, it is shown that results already available in the original E X B instability paper can be used to obtain an estimate of the striation scale size and onset time.

TABLE OF CONTENTS

LIST OF ILLUSTRATIONS

I. INTRODUCTION

We have previously reported[1] the development of an analytic model for the slow diffusive growth in time of a barium cloud. This model assumed a background ionosphere which was highly conducting but no longer infinitely so. This generalization of previous work[2] allowed polarization charges to accumulate on the cloud and thus permitted the cloud's shape to distort away from a gaussian ellipsoid. In Section II of this report, we give details of numerical calculations of this effect and present some illustrations of it. We are also able to make a crude estimate of the time required for appreciable steepening to occur. This is described in Section III.

In an earlier technical report[3] we also described numerical solutions of the linearized equations of motion of the cloud. These equations were linearized about the equilibrium gaussian ellipsoid derived in ref. 2. We also noted in this report that the particular numerical scheme used was rather inefficient and had been pushed close to its practical limit by the time the cloud had been represented by a 9 x 9 grid. We have now changed to an entirely different and much more efficient scheme. Details and illustrations of the results are given in Sect. IV. Finally,

Finally, we note that it is possible to make crude estimate of the scale size of striations and estimate their onset time by a simple extrapolation of results already in the original 1963 paper on the E X B instability.[4] Details are given in Sect. V.

II. NUMERICAL CALCULATION OF CLOUD DISTORTION

In the previous semi-annual[1], (hereafter referred to as I), an equation was derived for the growth by diffusion and convection of a cloud immersed in a highly conducting (but not infinitely conducting) background ionosphere. We also noted some typical numerical results. The purpose of this section is to further describe the numerical scheme used.

The basic equation is equation (17) of I.

$$\frac{\partial N}{\partial t} - \mathcal{D}_\perp \nabla_\perp^2 N + \frac{c}{B}\beta \nabla_\perp \cdot (N \underline{E}^{(1)}) + \frac{c}{B}(1-\alpha)\,\underline{b}\cdot \nabla N \times \underline{E}^{(1)} = 0 \tag{1}$$

where $N = N(\underline{R}_\perp, t)$

and $\underline{E}^{(1)}$, the first order correction (in the ratio of conductivities) to the electric field is given by equation (14) of I with t replaced by $t + \frac{a^2}{4\mathcal{D}_\perp}$:

$$\underline{E}^{(1)} = \frac{-e S_c}{2\pi \Sigma_B R^2}\left\{ \underline{i}_R \left[\frac{R^3}{4\mathcal{D}_\perp t'^2} \exp\left(\frac{-R^2}{4\mathcal{D}_\perp t'}\right) + \frac{B\mu_\perp^+}{c}\left[(\Omega\tau)_+^{-1} \underline{u}_0 \underline{n} + \underline{u}_c \times \underline{b}\cdot\underline{n}\right]\frac{\partial}{\partial R}\left[1 - \left(1 + \frac{R^2}{4\mathcal{D}_\perp t'}\right)\right.\right.\right. \tag{2}$$

$$\left.\left.\left. \exp\left(\frac{-R^2}{4\mathcal{D}_\perp t'}\right)\right]\right]^{R} - \frac{B\mu_\perp^+}{c}\left[(\Omega\tau)_+^{-1}\underline{u}_0 + \underline{u}_c \times \underline{b}\right] \cdot \left[1 - \exp\left(\frac{-R^2}{4\mathcal{D}_\perp t'}\right)\right]\right\}$$

where $t' = t + a^2/4D_\perp$.

The initial state is assumed to have a Gaussian profile of width a, and is normalized to the total number of particles S_c:

$$N(\underline{r}_\perp, 0) = \frac{S_c}{\pi a^2} e^{-r^2/a^2} \qquad (3)$$

To proceed further, we must fix a coordinate system. We assume that the external electric field E_c points in the positive y direction, the magnetic field in the positive z direction, and hence the E X B drift is in the positive x direction. (We remind the reader that the equations are expressed in coordinates which move with respect to the rest frame of the neutrals with velocity equal to the 0'th order drift given by

$$\underline{v} = -(\alpha-1)\,\underline{u}_o - \beta\,\underline{u}_o \times \underline{b}$$

cf. equation (12) of I)

We also reduce the equation to nondimensional form by measuring length in units of the initial Gaussian radius and time in units of $a^2/4D_\perp$:

$$r = r/a$$
$$T = t\,(4D_\perp/a^2) \qquad (4)$$

Substituting (2) into (1), specializing to our coordinate system and using (4), we obtain our basic equation

$$\frac{\partial N}{\partial t} - \frac{i}{4}\nabla_\perp^2 N + A(x,y,t)\,N + B(x,y,t)\,\frac{\partial N}{\partial x} + C(x,y,t)\,\frac{\partial N}{\partial y} = 0 \qquad (5)$$

where the coefficients are given by:

$$A \equiv \frac{\bar{\lambda}}{(1+\Gamma)^2}\left[\frac{x^2+y^2}{1+\Gamma} - 1 + \frac{\gamma}{2}\left[y - (\Omega\tau)_+^{-1}x\right]\right] \times EXP\ \frac{-(x^2+y^2)}{1+\Gamma}$$

$$B \equiv -\frac{\bar{\lambda}}{2}\left[\left(\frac{i}{(1+\Gamma)^2} + \frac{\gamma}{2(1+\Gamma)}\,\frac{y-(\Omega\tau)_+^{-1}x}{x^2+y^2}\right) \times \right.$$

$$\times (x+(\Omega\tau)_+ y)\, EXP\,\frac{-(x^2+y^2)}{1+\Gamma} - \frac{\gamma\,(1+(\Omega\tau)_+^2)\,(x^2-y^2)}{4\,(\Omega\tau)_+\,(x^2+y^2)^2} \times$$

$$\left.\times\left(EXP\,\frac{-(x^2+y^2)}{1+\Gamma} - 1\right)\right]$$

$$C \equiv -\frac{\bar{\lambda}}{2}\left[\left(\frac{i}{(1+\Gamma)^2} + \frac{\gamma}{2(1+\Gamma)}\,\frac{y-(\Omega\tau)_+^{-1}x}{x^2+y^2}\right)\left(y-(\Omega\tau)_+ x\right) \times\right.$$

$$\times EXP\,\frac{-(x^2+y^2)}{1+\Gamma} - \frac{\gamma\,(1+(\Omega\tau)_+^2)\,2xy}{4\,(\Omega\tau)_+\,(x^2+y^2)^2} \times$$

$$\left.\times\left(EXP\,\frac{-(x^2+y^2)}{1+\Gamma} - 1\right)\right]$$

(6)

In the above we have neglected terms of order $(\Omega\tau)_+ / (\Omega\tau)_-$ so that $\frac{c}{B}(1-\alpha) \rightarrow (\Omega\tau)_i / \mu_\perp^+$ and $\frac{c\beta}{B} \rightarrow \mu_\perp^+$.

In addition we have defined the two parameters:

$$\bar{\lambda} \equiv \frac{e S_0 \mu_\perp^+}{\Sigma_B a^2 \pi}$$

which is the ratio of the cross-cloud conductivity to that of the background and

$$\gamma \equiv \frac{e E_c a}{\kappa (T_+ + T_-)}$$

which is the normalized external electric field strength. The solution therefore depends only upon the specification of the three parameters $(\Omega\tau)_+$, $\bar{\lambda}$ and γ.

Numerical solutions to equation (5) have been obtained using the alternating direction implicit scheme (A.D.I). In this method the differential equation (5) is replaced by the following two coupled finite difference equations.

$$\frac{N_{i,j}^{m+1} - N_{i,j}^{m}}{\Delta T} = \frac{1}{4}\left(\frac{N_{i+1,j}^{m+1} + N_{i-1,j}^{m+1} - 2N_{i,j}^{m+1}}{(\Delta x)^2}\right) + \frac{1}{4}\left(\frac{N_{i,j+1}^{m} + N_{i,j-1}^{m} - 2N_{i,j}^{m}}{(\Delta y)^2}\right) - A N_{i,j}^{m+1} - B\left(\frac{N_{i+1,j}^{m+1} - N_{i-1,j}^{m+1}}{2\Delta x}\right) - C\left(\frac{N_{i,j+1}^{m} - N_{i,j-1}^{m}}{2\Delta y}\right) \qquad (7a)$$

$$\frac{N_{i,j}^{n+2} - N_{i,j}^{n+1}}{\Delta T} = \frac{1}{4}\left(\frac{N_{i+1,j}^{n+1} + N_{i-1,j}^{n+1} - 2N_{i,j}^{n+1}}{(\Delta x)^2}\right)$$

$$+ \frac{1}{4}\left(\frac{N_{i,j+1}^{n+2} + N_{i,j-1}^{n+2} - 2N_{i,j}^{n+2}}{(\Delta y)^2}\right) - A\,N_{i,j}^{n+1}$$

$$- B\left(\frac{N_{i+1,j}^{n+1} - N_{i-1,j}^{n+1}}{2\Delta x}\right) - C\left(\frac{N_{i,j+1}^{n+2} - N_{i,j-1}^{n+2}}{2\Delta y}\right) \qquad (7b)$$

where n refers to the time step and i and j to the grid point in x and y respectively.

Notice that in the first equation (7a) the differences in x are advanced one time step, whereas in the second the differences in y are advanced one step. (The coefficients A, B, and C are evaluated "in the middle", that is they are evaluated at $t = (n+1)\Delta t$ for both equations.)

This method can be shown to be much more stable than explicit schemes in which all spatial differences are taken at the present, known, time step. (For the case $\lambda = 0$, A.D.I. gives an unconditionally stable solution). On the other hand, the method is computationally much simpler than a completely implicit scheme in which the differences in both x and y are advanced at the same time. The reason, as can readily be seen from equation (7), is that the set of equations to be solved at each time step are tridiagonal in form and are thus susceptible to solution by a very

economical algorithm. We have used a double precision subroutine which employs Gaussian elimination with partial pivoting.

We set up the equations on a square grid, choosing $\Delta x = \Delta y = .20834$, which proved sufficiently small to guarantee accuracy, and ΔT as large as possible while still ensuring stability. Some error was inevitably introduced by the use of a finite sized grid for a problem which is defined on an infinite plane. We adopted the scheme of setting all of the grid boundary points to zero at each time step. For several of the runs in which the cloud diffused rapidly, we used an expanding grid scheme, that is as time developed and the cloud grew, we increased the overall size of the grid. In all cases the value of the density at the boundary points was no greater than five orders of magnitude less than the maximum value of the density.

In general, errors arose from three sources:

1.) truncation error due to the finite grid spacing,

2.) machine round-off error, and

3.) error due to the finite size of the grid.

The first was checked by choosing different values of grid spacing; the second by using two compilers, one which rounds off to the next larger integer and the other to the smaller;

and the third by varying the grid size. The resulting errors from all causes are less than 10%.

Some computer results are shown in Figs. 1-5. In all cases, we set $\bar{\lambda} = 0.1$, $\gamma = 20$ and varied $(n\tau)_4$. The grid scale in these plots is in kilometers with $a = 4.8$ km. To get some idea of the real time corresponding to the various values of T used, note that $D_\perp \cong .045$ km^2/s (Secede 1, Dogwood) and thus $t(\text{real}) = (a^2/4D_\perp)T \cong 127\,T$ seconds. Note the thinning and indentation on the front side of the cloud and the steepening in the rear. The arrow marked u_c represents the actual direction of drift of the cloud relative to the neutrals. Note the symmetrical distortion of the cloud in the large limit. This symmetry is readily verified by examination of the coefficients in Eq. (6) in this limit. The leading terms in B are proportional to x^2 and y^2 while those in C are proportional to xy.

III. ESTIMATE OF STEEPENING TIME

One may also obtain a crude estimate of the "steepening time" by examining the coefficients in Eq. (6). In the large $(\Omega\tau)_+$ limit, the leading terms are in coefficients $\mathcal{B}$ and $\mathcal{C}$ and are of order

$$\simeq \frac{1}{4}\bar{\lambda}\gamma(\Omega\tau)_+$$

Hence the distortion time T_D is

$$T_D \simeq \frac{4}{\bar{\lambda}\gamma(\Omega\tau)_+} \qquad (8)$$

This is in units of the diffusion time $a^2/4D_\perp$. In real time, we have

$$T_D \simeq \frac{a^2}{4D_\perp}\cdot\frac{4}{\bar{\lambda}\gamma(\Omega\tau)_+} = \frac{a}{u_0\bar{\lambda}} \qquad (9)$$

IV. NEW NUMERICAL RESULTS FOR THE LINEAR INSTABILITY EIGENFUNCTIONS

A: Linear Equation:

Some preliminary numerical calculations of the fastest growing linear eigenvalues were presented in an earlier semiannual report.[3] We now have changed to a much improved numerical scheme and report considerably changed results on much larger grids. The starting point for this calculation is the same set of equations as shown in Eq. (2.10) of ref. 3 above. These are

$$\left[\omega + (\pi/2z_c)^2 \mathcal{D}_{\parallel}\right] \bar{N}\chi - D_{\perp}^{\pm} \nabla_{\perp}^2 (\bar{N}\chi)$$

$$\mp \mu_{\perp}^{\pm} \nabla_{\perp} \cdot (A\chi \nabla_{\perp} N + \bar{N} \nabla_{\perp} \varphi) \pm \mu_{\parallel}^{\pm} \tfrac{1}{2} \chi \times$$

$$\times \left[C \nabla_{\perp}^2 \bar{N} - K \underset{\sim}{E}_0 \cdot \nabla_{\perp} \bar{N} - L \underset{\sim}{E}_0 \times \underset{\sim}{b} \cdot \nabla_{\perp} \bar{N}\right]$$

$$- (\Omega\tau)_{\pm} \mu_{\perp}^{\pm} \underset{\sim}{b} \cdot \left[A \nabla_{\perp}\chi \cdot \nabla_{\perp}\bar{N} + \nabla_{\perp}\bar{N} \times \nabla_{\perp}\varphi\right]$$

$$+ \left[-\frac{c}{B}\beta \pm \mu_{\perp}^{\pm}\right] \underset{\sim}{E}_0 \cdot \nabla(\bar{N}\chi)$$

$$+ \left[\frac{c}{B}(\alpha - 1) + (\Omega\tau)_{\pm} \mu_{\perp}^{\pm}\right] \underset{\sim}{E}_0 \times \underset{\sim}{b} \cdot \nabla_{\perp} (\bar{N}\chi) = 0 \qquad (10)$$

where we have replaced

$$\underset{\sim}{E}_{\perp}^{(0)} \longrightarrow -A\,\frac{\nabla_{\perp}\bar{N}}{\bar{N}}$$

$$\underset{\sim}{\mathcal{E}}_{\perp} \longrightarrow -\nabla\varphi$$

and redefined

$$K \equiv \frac{c}{B}H$$

$$L \equiv -\frac{c}{B}G$$

Otherwise, all symbols have the same significance as in ref. 3. Next we reduce this equation to dimensionless form by defining

$$\underset{\sim}{R} \equiv \underset{\sim}{R}/a$$

$$\omega \equiv \omega t$$

$$\varphi \equiv \varphi/A$$

$$\gamma \equiv \frac{e E_0 a}{K(T_+ + T_-)}$$

$$T \equiv t\,\frac{4\nu_L}{a^2}.$$

and further simplify by dropping terms of order $(\Omega\tau)_+/(\Omega\tau)_-$ (consistent with our expansion in powers of $D_{\parallel}^{+}/D_{\parallel}^{-}$). The resultant equation in Cartesian coordinates, with $\underset{\sim}{E}_0$ in the positive y-direction, is:

$$A^{\pm}\nabla_{\perp}^2\chi + B^{\pm}\frac{\partial\chi}{\partial x} + C^{\pm}\frac{\partial\chi}{\partial y} + D^{\pm}\chi$$
$$+ E^{\pm}\frac{\partial\varphi}{\partial x} + F^{\pm}\frac{\partial\varphi}{\partial y} + G^{\pm}\nabla_{\perp}^2\varphi = \omega\chi \qquad (11)$$

where

$$A^{\pm} \equiv \frac{T}{4}\left(1+\frac{T_+}{T_-}\right)^{-1} f^{\pm}\,\frac{T_{\pm}}{T_-}.$$

$$B^{\pm} \equiv \frac{T}{4}\left(1+\frac{T_+}{T_-}\right)^{-1} f^{\pm}\left[\left(\frac{2T_\pm}{T_-}\pm 1\right)\frac{1}{\bar N}\frac{\partial \bar N}{\partial x} + \right.$$

$$\left. + (\Omega T)_\pm \frac{1}{\bar N}\frac{\partial \bar N}{\partial y}\right] \pm \frac{T}{4}\,\delta\,\frac{1}{(\Omega T)_\mp}$$

$$C^{\pm} \equiv \frac{T}{4}\left(1+\frac{T_+}{T_-}\right)^{-1} f^{\mp}\left[\left(\frac{2T_\pm}{T_-}\pm 1\right)\frac{1}{\bar N}\frac{\partial \bar N}{\partial y} - (\Omega T)_\pm \frac{1}{\bar N}\frac{\partial \bar N}{\partial x}\right] \mp \frac{T}{4}\,\delta\,\frac{(\Omega T)_\pm}{(\Omega T)_-}$$

$$D^{\pm} \equiv -\frac{\pi^2}{16 z_0^2}\, T\left[1+(\Omega T)_+^2\right] + \frac{T}{16}(3\pm 1)\frac{\nabla_\perp^2 \bar N}{\bar N}$$

$$+ \frac{T\delta}{4}\left[\mp\frac{(\Omega T)_\pm}{2(\Omega T)_-}\,\frac{1}{\bar N}\frac{\partial \bar N}{\partial y} \pm \frac{1}{2(\Omega T)_\mp}\,\frac{1}{\bar N}\frac{\partial \bar N}{\partial x}\right].$$

$$E^{\pm} = \frac{T}{4}\left(1+\frac{T_+}{T_-}\right)^{-1} f^{\mp}\left(\pm\frac{1}{\bar N}\frac{\partial \bar N}{\partial x} - (\Omega T)_\pm \frac{1}{\bar N}\frac{\partial \bar N}{\partial y}\right)$$

$$F^{\pm} = \frac{T}{4}\left(1+\frac{T_+}{T_-}\right)^{-1} f^{\pm}\left(\pm\frac{1}{\bar N}\frac{\partial \bar N}{\partial y} + (\Omega T)_\pm \frac{1}{\bar N}\frac{\partial \bar N}{\partial x}\right).$$

$$G^{\pm} = \pm\frac{T}{4}\left(1+\frac{T_+}{T_-}\right)^{-1} f^{\pm}$$

(12)

and $$f^{\mp} \equiv \frac{\mu_\pm}{\mu_\perp^+} = 1 \quad \text{upper sign}$$

$$= \frac{1+(\Omega T)_+^2}{(\Omega T)_-(\Omega T)_+} \quad \text{lower sign}$$

We take $\bar N$ to have a gaussian radius $\underline{a}$ at the origin of time. Thus

$$\bar N \sim \exp\left[-r^2/(1+T)\right]$$

B: Numerical Scheme:

The two coupled equations above can be written in the form:

$$L_1^+ \chi + L_2^+ \varphi = \omega \chi \qquad (13a)$$

$$L_1^- \chi + L_2^- \varphi = \omega \chi \qquad (13b)$$

If one replaces the differential operators by the finite difference approximation,

$$\nabla^2 \psi \rightarrow \frac{\psi_{i+1,j} + \psi_{i-1,j} + \psi_{i,j+1} + \psi_{i,j-1} - 4\psi_{i,j}}{(\Delta x)^2}$$

$$\frac{\partial \psi}{\partial x} \rightarrow \frac{\psi_{i+1,j} - \psi_{i-1,j}}{2\Delta x} \qquad (14)$$

$$\frac{\partial \psi}{\partial y} \rightarrow \frac{\psi_{i,j+1} - \psi_{i,j-1}}{2\Delta x}$$

the operators $L_1^{\pm}$ and $L_2^{\pm}$ become matrix operators. The set of equations are closed by specifying homogeneous boundary conditions on χ and φ. If we now subtract Eq. (13b) from (13a) we obtain

$$(L_2^{+} - L_2^{-})\varphi = -(L_1^{+} - L_1^{-})\chi \qquad (15)$$

Assuming $(L_2^{+} - L_2^{-})$ is nonsingular, we can invert the matrix and substitute the resulting equation for φ back into (13a). We can then solve (13a) for the eigenvalue and eigenfunction by any of a number of algorithms.

This straightforward procedure was the method originally employed for this problem[3]. Unfortunately, it suffers from the limitation of being very uneconomical. To see this we observe that an $n \times n$ grid has n^2 points. (When we refer to the dimensions of a grid, we do not consider the boundary points which do not enter the matrix equations due to the homogenous boundary conditions on χ and φ). Eq. (13) includes one equation for each point and hence the coefficient matrices

will be arrays of dimension m^2 by m^2 for a total of m^4 elements. The storage requirements of the computer therefore increases as the fourth power of the grid dimension and the method very quickly outgrows the capacity of the computer. Indeed it was found[3] to be impossible to consider grids with more than 11 x 11 points. This is hardly a sufficiently fine mesh to discern the complicated structure of an unstable mode.

To obtain a more economical procedure, we first observe that most of the elements in the matrices of coefficients are zero. Indeed, it is clear from Eq. (14) that there are only 5 possible non-zero bands of elements running diagonally across each coefficient matrix; a total of at most only $5m^2$ non-zero elements. The problem enters in the solution of Eq. (15) since the inversion of the matrix $(\mathcal{L}_2^+ - \mathcal{L}_1^-)$ will in general destroy the band structure and produce a full matrix.

Our solution to this problem involved a double iterative procedure.* We solved equation (13a) for the eigenvalue and eigenvector χ iteratively via the power method[5], obtaining φ for each iterate by solving the set of equations (15). That is, an initial approximation for χ was randomly generated and substituted into the R.H.S. of equation (15). The resulting set of inhomogeneous linear equations was solved for φ using point successive overrelation[6], a variation of the usual Gauss-Seidel with a parameter to accelerate convergence.

The result for φ was substituted into (13a) and a new iterate for χ was obtained using the power method. This was substituted back into the R.H.S. of Eq. (15) and then the process was continued.

This process in general converges to the eigenvector corresponding to the eigenvalue with largest absolute magnitude[5]. However, we desire the fastest growing eigenmode, that is the eigenmode whose eigenvalue has the largest real part. To obtain the latter eigenmode, we solved, in place of the original equation which takes the form

$$A\psi = \omega\psi$$

(A is a matrix operator), the equation:

$$(A + p\mathcal{I})\chi = \omega\chi \qquad (16)$$

where p is a real constant and $\mathcal{I}$ is the unit matrix. It is clear that if we kept all of the original eigenvalues in the complex plane, the effect of adding the $p\mathcal{I}$ term in Eq. (16) will be to shift all of the values parallel to the real axis by an amount p. One can readily show by geometrical arguments, that there always exists a value for the shift p which shifts the spectrum of eigenvalue such that the original eigenvalue (or complex conjugate pair of eigenvalues) with the largest real part becomes, after the shift, the one with the largest absolute value. The process will then converge to this eigenmode, and one can substract the shift p to obtain

the original value for the eigenvalue.

C: Results:

We have run a series of numerical solutions for grid sizes 13 x 13, 19 x 19, 25 x 25, 37 x 37 and 49 x 49. For the purpose of these runs we assumed the following parameter values:

$$(\Omega\tau)_+ = 5$$

$$\gamma = 2.0$$

$$z_0 = 50$$

$$\frac{T_-}{T_+} = 1.72$$

We also assumed that the grid covered three e-folding lengths of the equilibrium density, i.e. we assumed $R_0^2/(1+\tau) = 3$ where R_0 is the distance from the center of the grid along x (or y) to the edge.

Figures 6 - 9 show plots of the density ($n=\bar{N}/\chi$) for the four grids: 13 x 13, 19 x 19, 25 x 25, and 37 x 37 for the case $\tau = 2.0$ (the 49 x 49 grid converged too slowly for a reasonable result for the eigenvector; we have used only the result for the eigenvalue - see below). Notice that all four grids show striations along the lower left-hand corner of the cloud. The amplitude of the perturbation density throughout the rest of the cloud is smaller by at least three orders of magnitude compared with the maximum value in the striations.

Moreover, the striations are directed approximately parallel to the equilibrium drift velocity: $\underset{\sim}{u}_o = \mu_\perp^+ \underset{\sim}{E}_o + (\nabla T)_+ \mu_\perp^+ (\underset{\sim}{E}_o \times \underset{\sim}{b})$. Hence, they point out the rear end of the cloud, a result in accord with observation.

In Table 1 we list the eigenvalues corresponding to the eigenfunctions shown in figure 6-9. We observe that the eigenvalues are complex; but their real parts are of order ten times their imaginary parts.

The question of convergence to a unique eigenvalue is a matter of continuing concern. In figure 10 we plot the real part of the eigenvalue as a function of grid spacing Δx. One would hope that as $\Delta x \to 0$, the value of $Re\,\lambda$ would level off and achieve a constant value. Unfortunately, as can be seen from figure 10, even for a 49 x 49 grid this has not occurred. We therefore conclude that as we go to finer grids we are picking up even faster growing modes. To test whether this process converges, we plotted $\log \Delta x$ as a function of $Re\,\lambda$. If the curve were concave downward the process would converge whereas if it were concave upwards it would not. The results, displayed in figure 11 show the curve to be very slightly concave downward although the result does strain somewhat the allowed errors placed upon the data points.

V. Approximate Model for Estimating Striation Scale Size and Onset Time.

If one is willing to settle for use of a slab model to represent the cloud, it should be possible to use the results already present in Ref. 4. We shall show how to do this using simple approximations. All notation will follow that paper (including y being the magnetic field direction!)

The basic result in Ref. 4 is contained in Eq. (3.18). Let us now simplify by assuming that the most unstable mode is one with very long wavelength in the magnetic field direction. This is because y-variation leads only to damping. Hence letting $k_y^2 \to 0$ our result reduces to:

$$\omega_I = \frac{\Gamma \bar{n}_0 \Lambda^2 (\mu_\perp^+ + \mu_\perp^-) - \textcircled{H} k_z^2 (dn_0/dx)[\mu_\perp^+/(n\tau)_+]}{\bar{n}_0^2 \Lambda^4 (\mu_\perp^+ + \mu_\perp^-)^2 + k_z^2 (dn_0/dx)^2 [\mu_\perp^+/(n\tau)_+]^2}$$

where

$$\Gamma = -\bar{n}_0 \Lambda^4 (\mu_\perp^- D_\perp^+ + \mu_\perp^+ D_\perp^-)$$

$$\textcircled{H} = -\bar{E}_0 \bar{n}_0 \Lambda^2 \mu_\perp^- \mu_\perp^+ [(n\tau)_+ + (n\tau)_-] +$$

$$+ \frac{dn_0}{dx}\left\{\Lambda^2 (D_\perp^+ \mu_\perp^- (n\tau)_- - D_\perp^- \mu_\perp^+ (n\tau)_+) + \frac{\mu_\perp^+ \mu_\perp^-}{2} \frac{dE_0}{dx}[(n\tau)_+ + (n\tau)_-]\right\}$$

$$\Lambda^2 \equiv k_z^2 + (\pi/\ell)^2 .$$

where we already assumed $(n\tau)_- >> 1$. It is obvious that the second term in the denominator is small compared to the first

for $(\Omega\tau)_+ > 1$. Note that

$$\left(\frac{dn_0}{dx}\right)^2 < \left(\frac{\pi n_c}{\ell}\right)^2 < n_c^2 \Lambda^2$$

and

$$k_y^2 < \Lambda^2$$

Hence we drop this second term and also neglect $\mu_\perp^-$ compared to $\mu_\perp^+$.

Let us compare the three terms in ⑭ . The ratio of the first term to the second is:

$$\simeq \frac{\bar{E}_0 \bar{n}_c \mu_\perp^+}{D_\perp^+ (dn_c/dx)} \leq \frac{e \bar{E}_0 \ell}{k T_+}$$

We assume that this is large compared to unity (in most cases, it is of order 20 - 100). Hence, we neglect the second term. By the same means, the ratio of the first to the third is

$$\simeq \frac{\bar{E}_0 \bar{n}_0 \Lambda^2}{(d\bar{E}_0/dx)(dn_c/dx)} > \Lambda^2 \ell^2 > 1 .$$

Hence

$$⑭ \simeq - \bar{E}_0 \bar{n}_c \Lambda^2 \mu_\perp^+ \, e/B$$

The resulting expression for the growth rate is:

$$\omega_I = -\Lambda^2 \frac{\mu_\perp^- D_\perp^+ + \mu_\perp^+ D_\perp^-}{\mu_\perp^+} + \frac{c E_0}{B (n\tau)_+} \frac{k_y^2}{\Lambda^2} \frac{1}{n_c} \frac{dn_c}{dx} \quad (17)$$

The first term is recognized as the damping due to ambipolar diffusion in the perpendicular direction (the result of taking $k_y^2 = 0$); the second term is destabilizing if $\bar{E}_0 \frac{dn_c}{dx}$ is positive (the usual necessary condition for the E x B instability). There is a critical wavelength for given $\bar{E}_0$. To see this, note that the damping term is finite for $k_y^2 = 0$ and goes to

infinity as $k_3^2 \to \infty$. The destabilizing term goes to zero as $k_3^2 \to 0$ and goes to a constant value as $k_3^2 \to \infty$. A conceptual plot of these terms (for small E_0) is shown below.

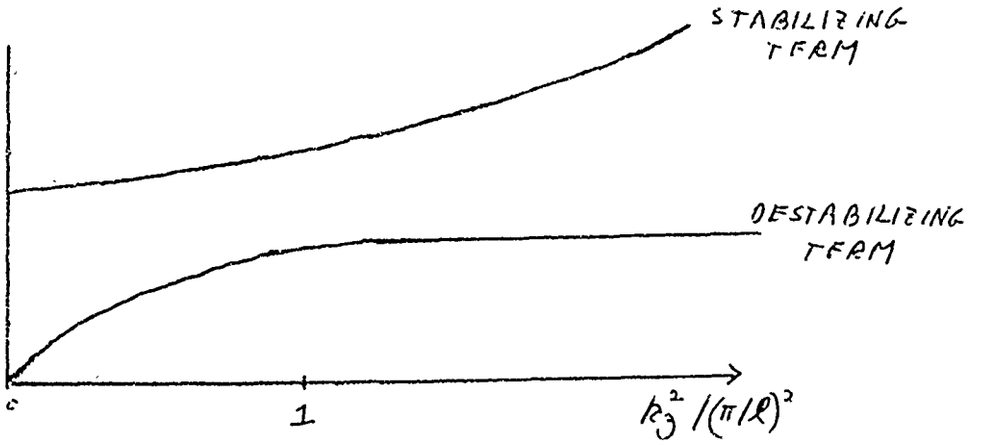

Note that there is stability in this case. As E_0 increases, the destabilizing term increases until the curves cross. This gives the threshold values of k_3^2 and E_0. From the shape of the curves and the fact that both have their turnover in the vicinity of $k_3^2 \cong (\pi/\ell)^2$ it is obvious that the threshold value of k_3^2 will be in the vicinity of $(\pi/\ell)^2$.

One can also view the onset of instability as a function of the growth in cloud size while holding E_0 fixed. Growth means that ℓ increases just as $\left(\frac{1}{M_c}\frac{dM_c}{dx}\right)^{-1}$ does. Thus as the cloud grows, the stabilizing term decreases at its lower end, while the destabilizing term increases at the lower end and decreases at the upper end. Again when the two terms cross, we have the critical wavelength and the critical size of the cloud (which can be related to an onset time for any given

theory or empirical set of values of cloud size as a function of time).

Note that in the derivation in Ref. 4, the length ℓ represents a distance in the direction of the density gradient over which the perturbation extends in that direction. It is assumed small compared to the density gradient itself. It may be possible to get useful estimates of scale size and onset times by arbitrarily assuming

$$\ell \cong \frac{1}{5}\left(\frac{1}{n_0}\frac{dn_0}{dx}\right)^{-1}$$

For example, if we set $k_3^2 = (\pi/\ell)^2$ and use the estimate above, it is easy to calculate the critical scale size from Eq. (17). Equaling the two terms on the r.h.s., one has

$$2\left(\frac{\pi}{\ell}\right)^2 D_\perp^- \left(1+\frac{T_+}{T_-}\right) = \frac{\epsilon E_0}{B(nT)_+}\frac{1}{2d}$$

where

$$d = \left(\frac{1}{n_0}\frac{dn_c}{dx}\right)^{-1}$$

Now

$$\ell \cong d/5$$

Hence

$$d_{crit} \cong 4\pi^2(25)\frac{D_\perp^- B(nT)_+}{\epsilon E_0}\left(1+\frac{T_+}{T_-}\right)$$

$$\cong \frac{100\pi^2}{u_0}\frac{D_\parallel^-}{(nT)_-}\left(1+\frac{T_+}{T_-}\right)\frac{T_-}{T_+}$$

where

$$u_0 \equiv \frac{\epsilon E_0}{B}$$

If we take typical values:

$$D_{\parallel}^{T} \cong 10^{5} \ m^2/sec.$$

$$u_0 \cong 20 \ m/sec.$$

$$T_+'/T_- \cong 1/2$$

we obtain

$$d_{crit} \cong \frac{1.5 \times 10^{4}}{(\Omega\tau)_-} \ km.$$

A very crude estimate, of course, but not entirely unreasonable since $(\Omega\tau)_- \cong 10^{4}$.

ACKNOWLEDGMENT

*The authors are indebted to B. L. Buzbee of the Los Alamos Scientific Laboratories Numerical Analysis Division for suggesting this approach.

REFERENCES

1. Albert Simon and Arthur M. Sleeper, RADC-TR-71-106 March 15, 1971.

2. Albert Simon, J. Geophys. Res. 75, 6287 (1970). See also RADC-70-27, Feb. 1970.

3. Albert Simon, RADC-TR-70-208, Sept. 1970.

4. A. Simon, Phys. Fluids 6, 382 (1963).

5. J. H. Wilkinson, The Algebraic Eigenvalue Problem, Claredon Press, Oxford, England, 1965 pp. 570-584.

6. Richard S. Varga, Matrix Iterative Analysis, Prentice Hall, Inc., Englewood Cliffs, N.J., 1962, Chap. 3.

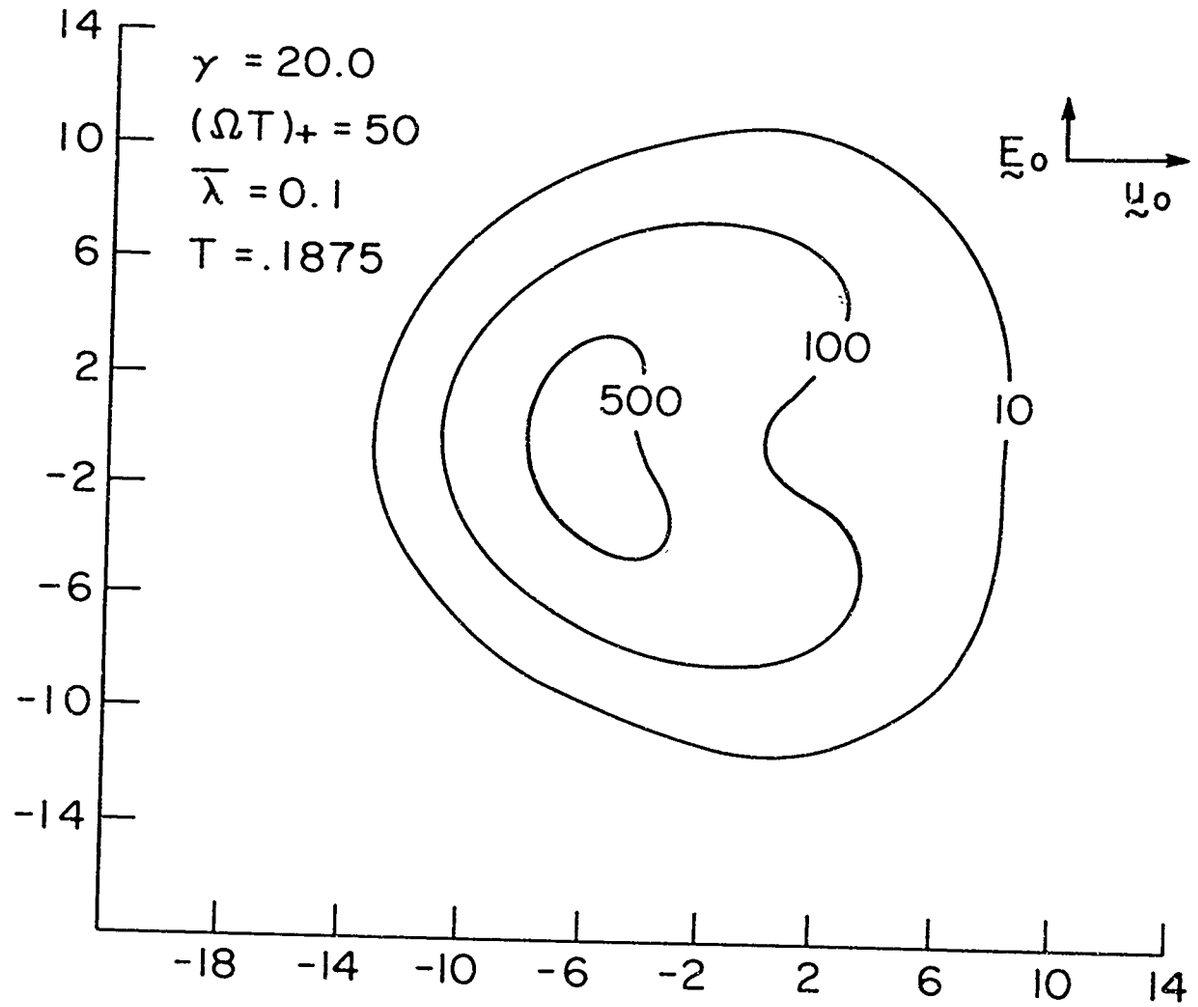

FIG. 1 DENSITY CONTOURS FOR $(\Omega T)_+ = 50$ AT $T = .1875$

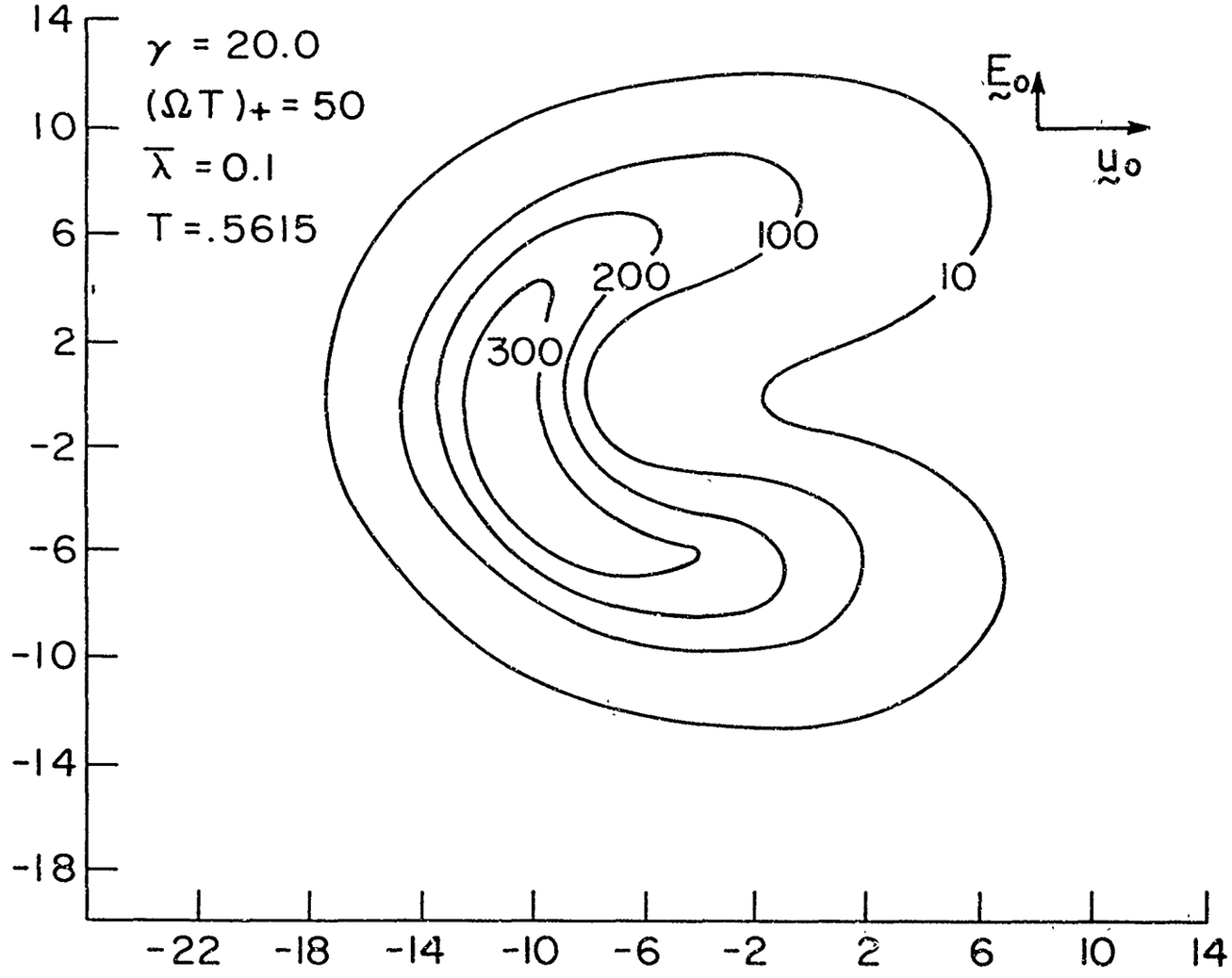

FIG. 2 DENSITY CONTOURS FOR (ΩT)+ = 50 AT T = .5615

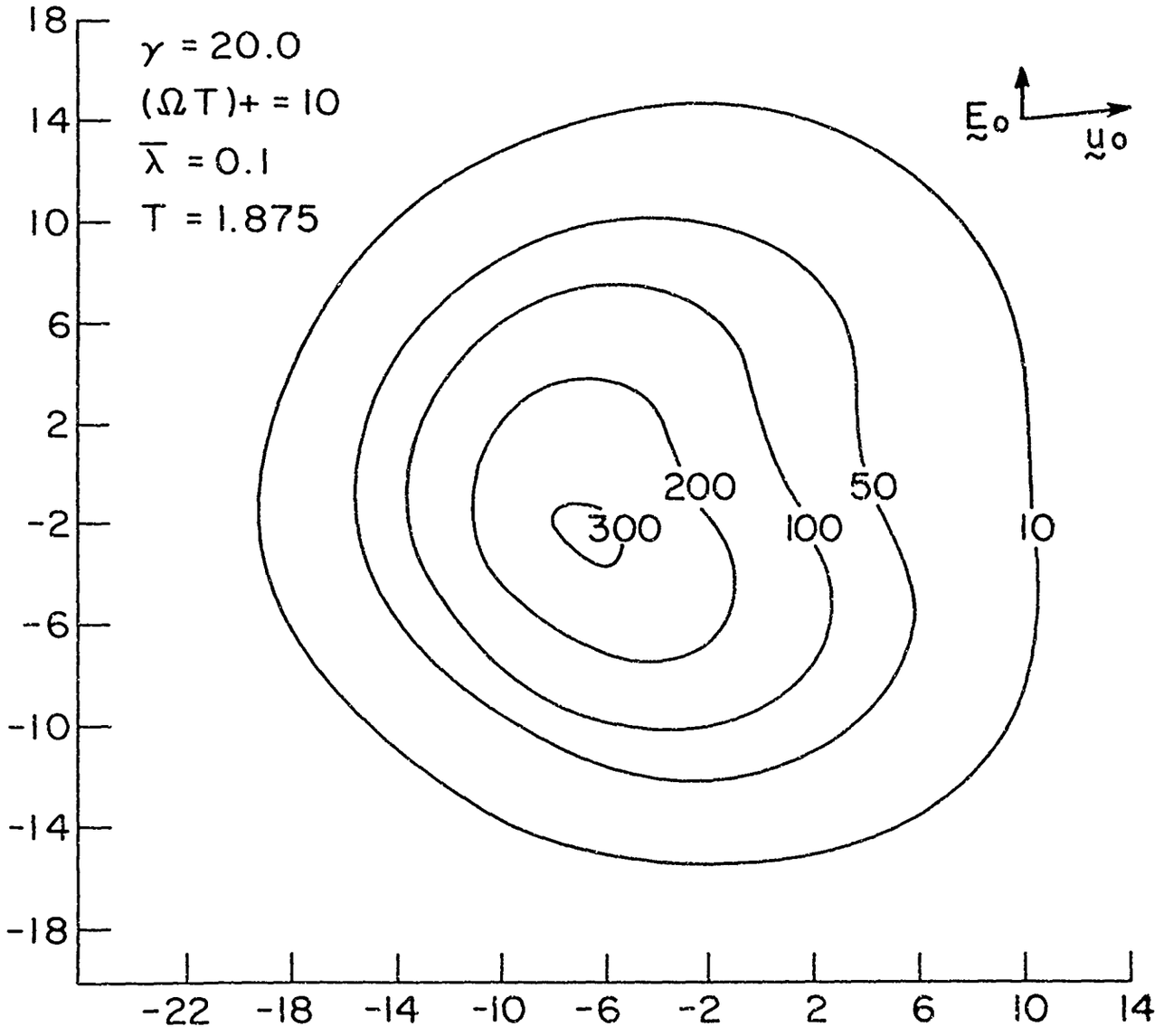

FIG. 3 DENSITY CONTOURS FOR $(\Omega T)_+ = 10.0$ AT $T = 1.875$

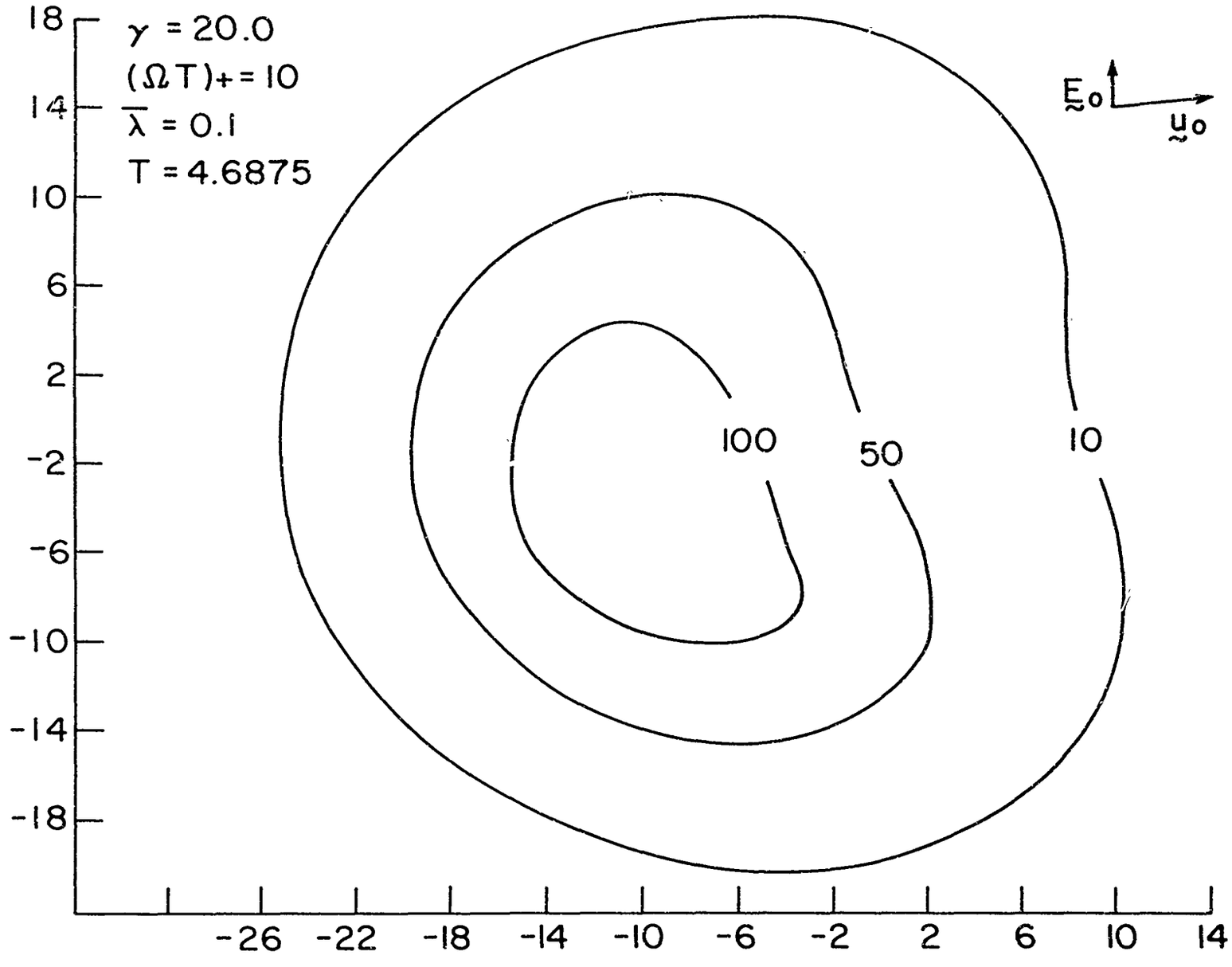

FIG. 4 DENSITY CONTOURS FOR $(\Omega T)_+ = 10.0$ AT $T = 4.6875$

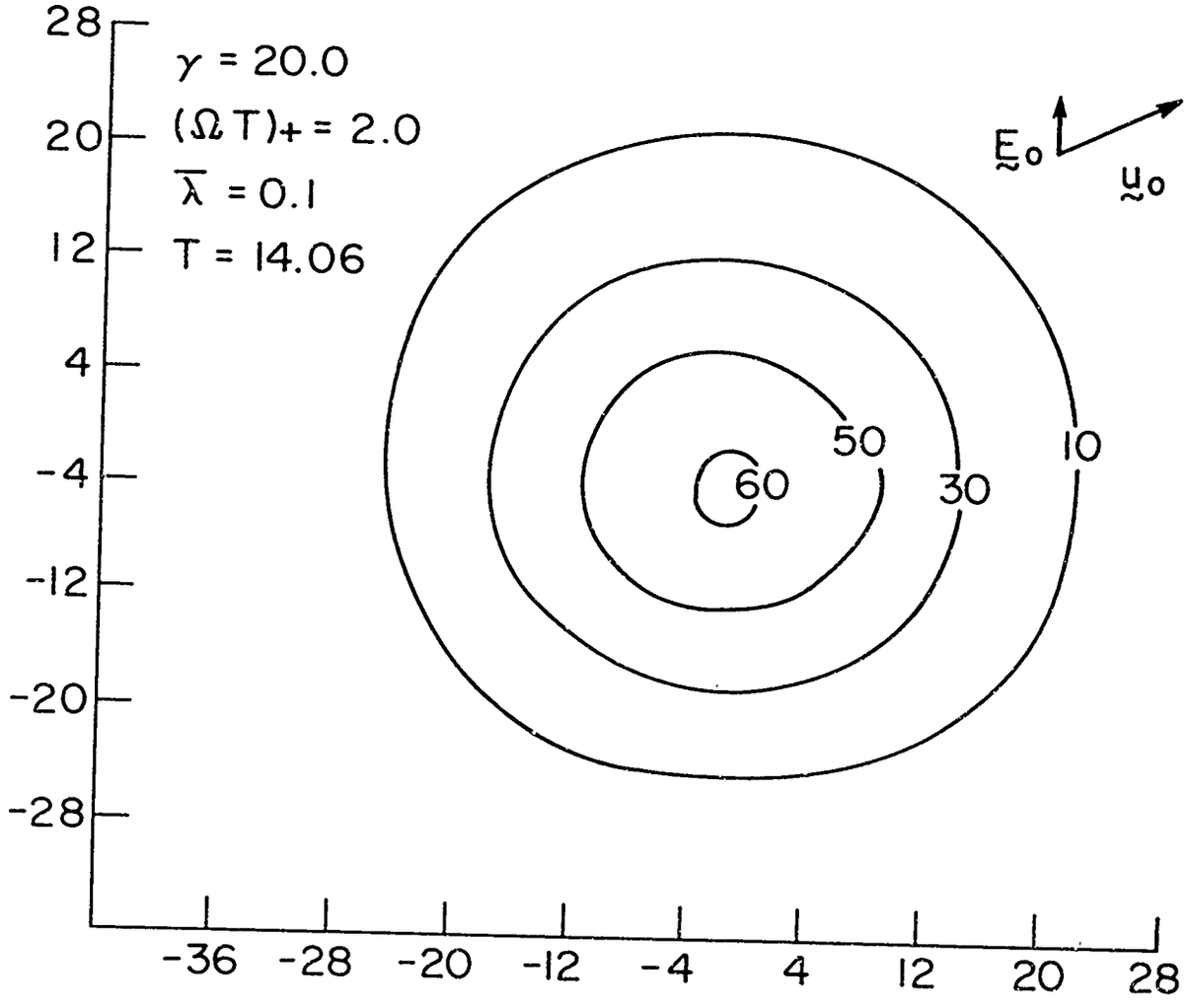

FIG. 5 DENSITY CONTOURS FOR $(\Omega T)_+ = 2.0$ AT $T = 14.06$

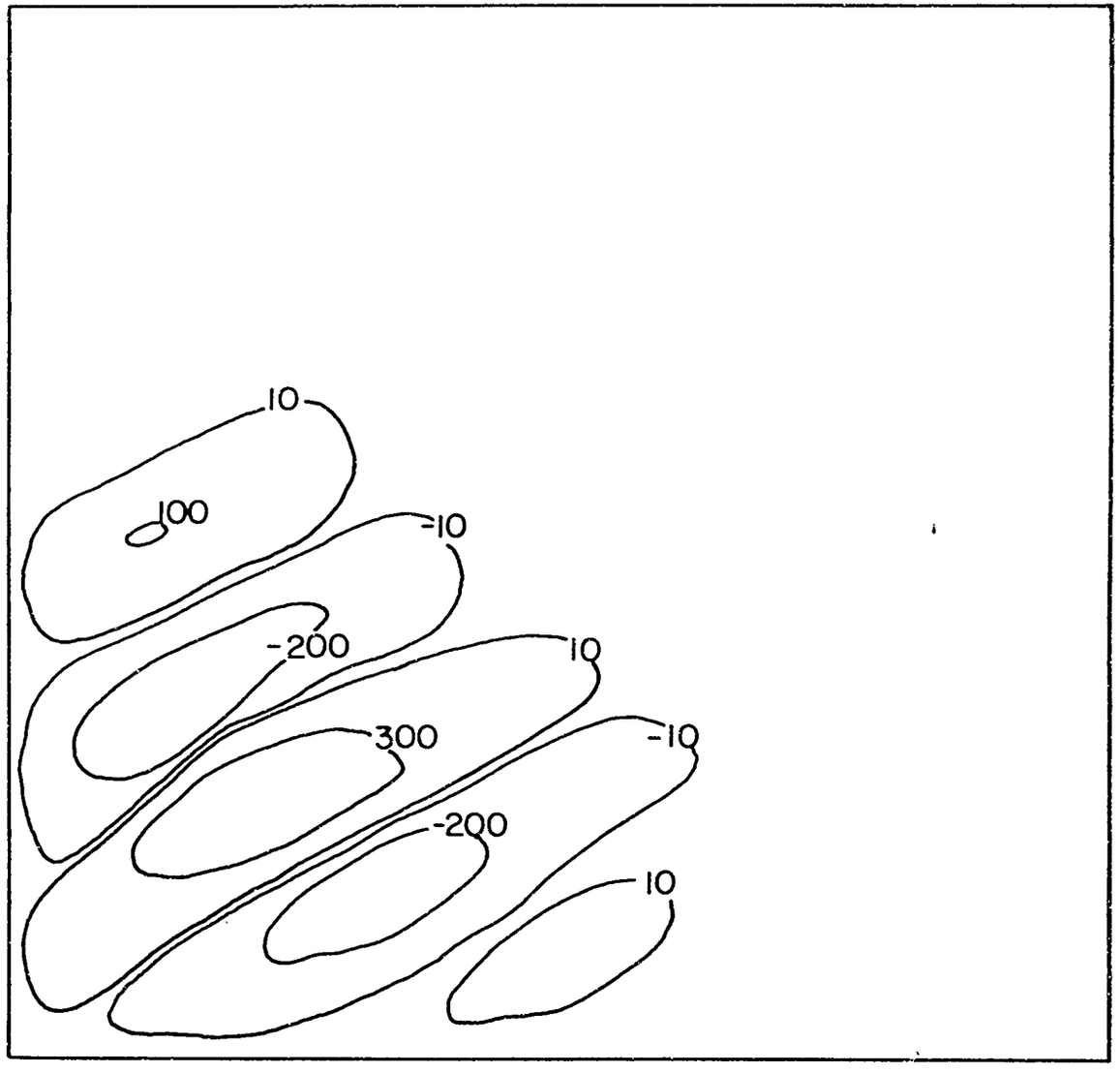

FIG. 6 DENSITY PERTURBATIONS 13x13 GRID

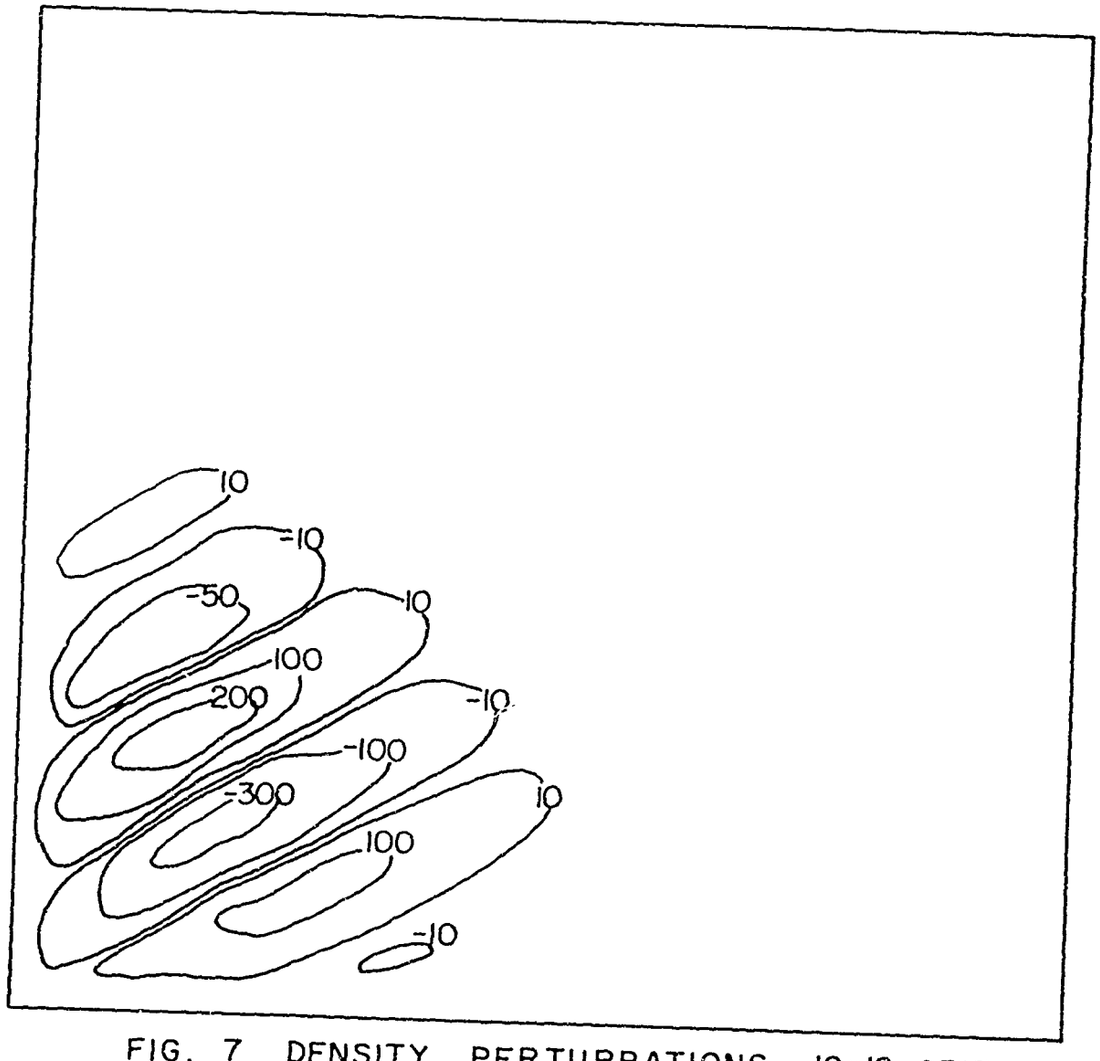

FIG. 7 DENSITY PERTURBATIONS 19x19 GRID

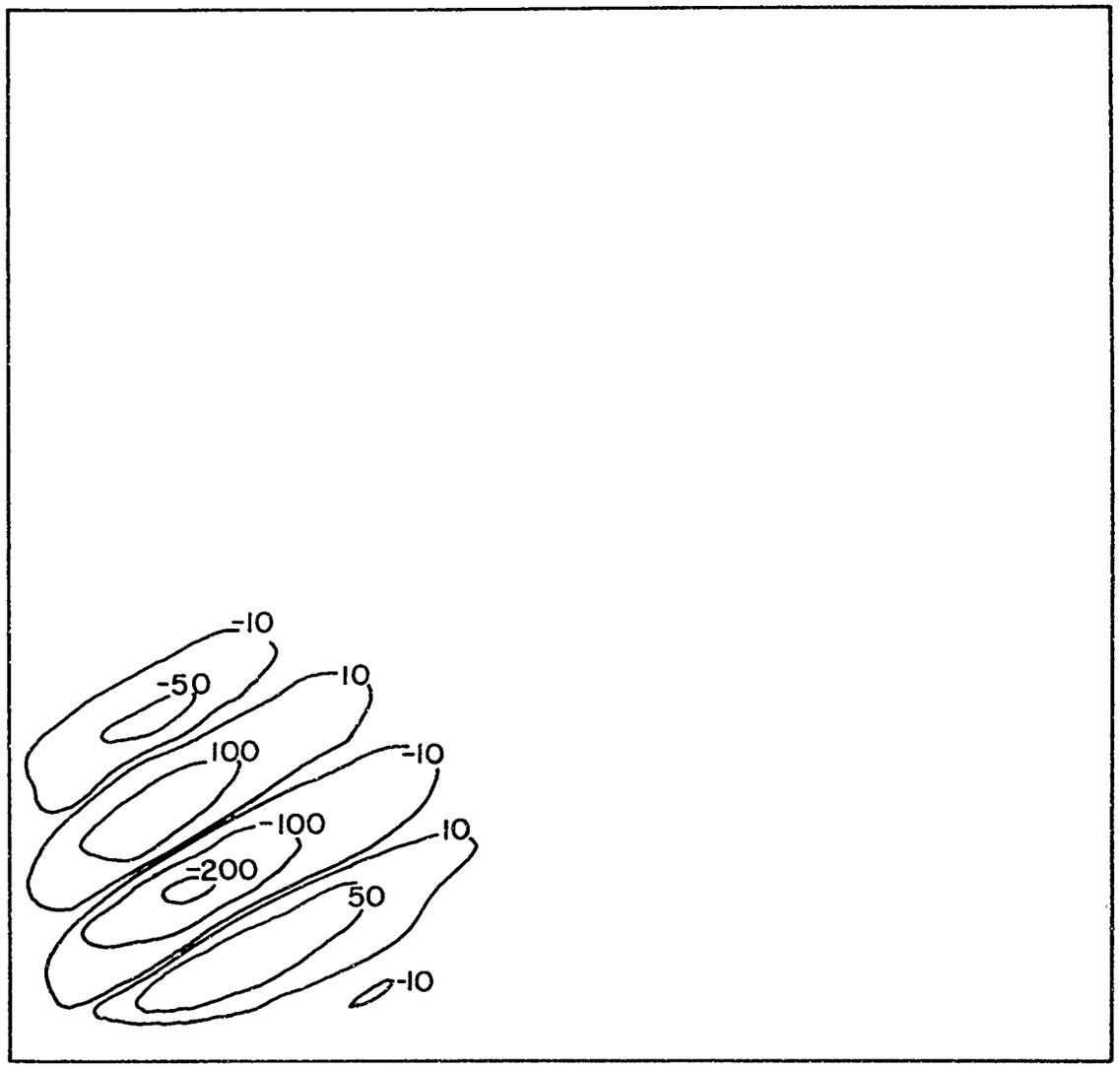

FIG. 8 DENSITY PERTURBATIONS 25 x 25 GRID

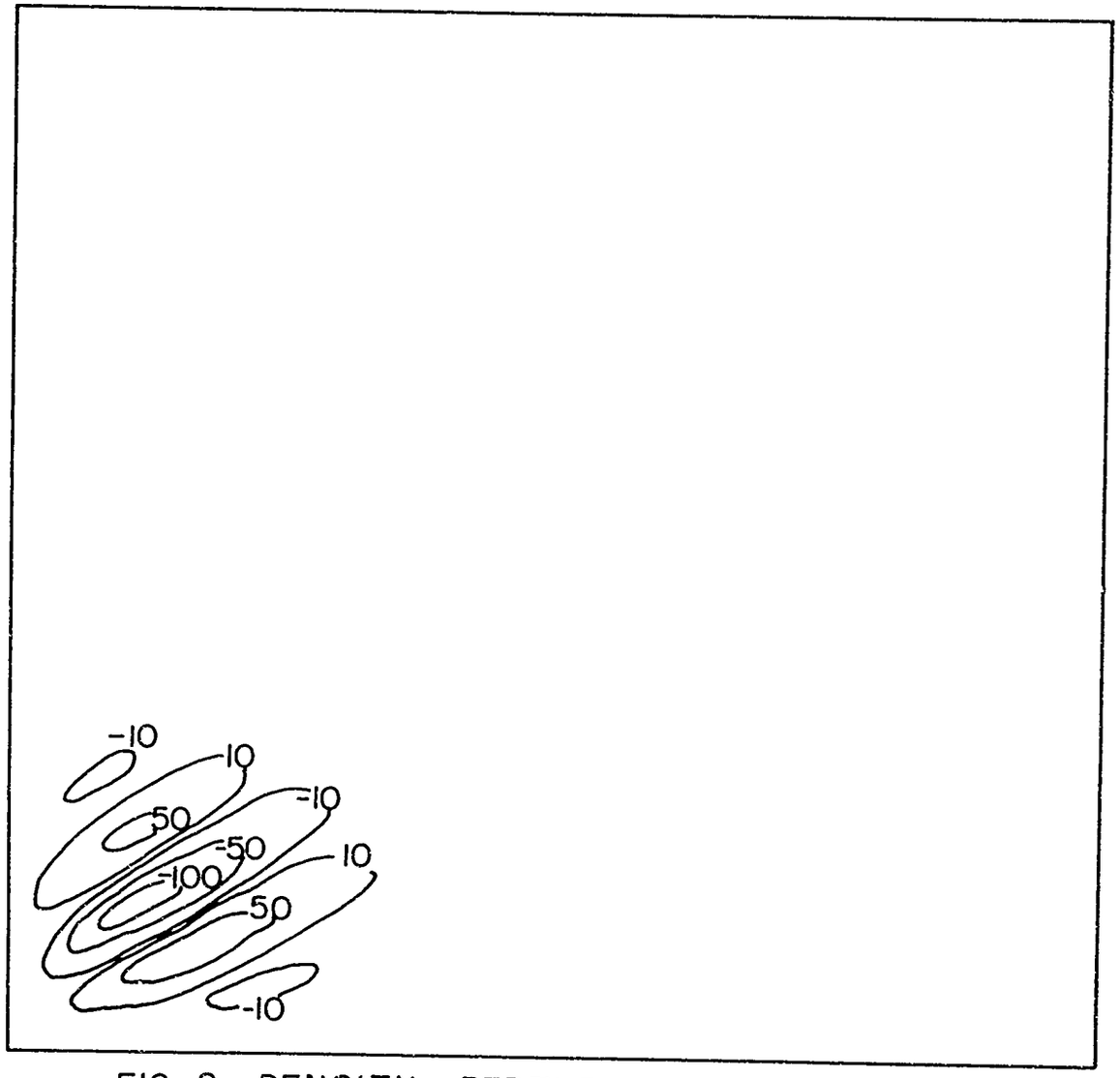

FIG. 9 DENSITY PERTURBATIONS 37x37 GRID

FIG. 10

THE REAL PART OF λ AS A FUNCTION OF GRID SPACING ΔX

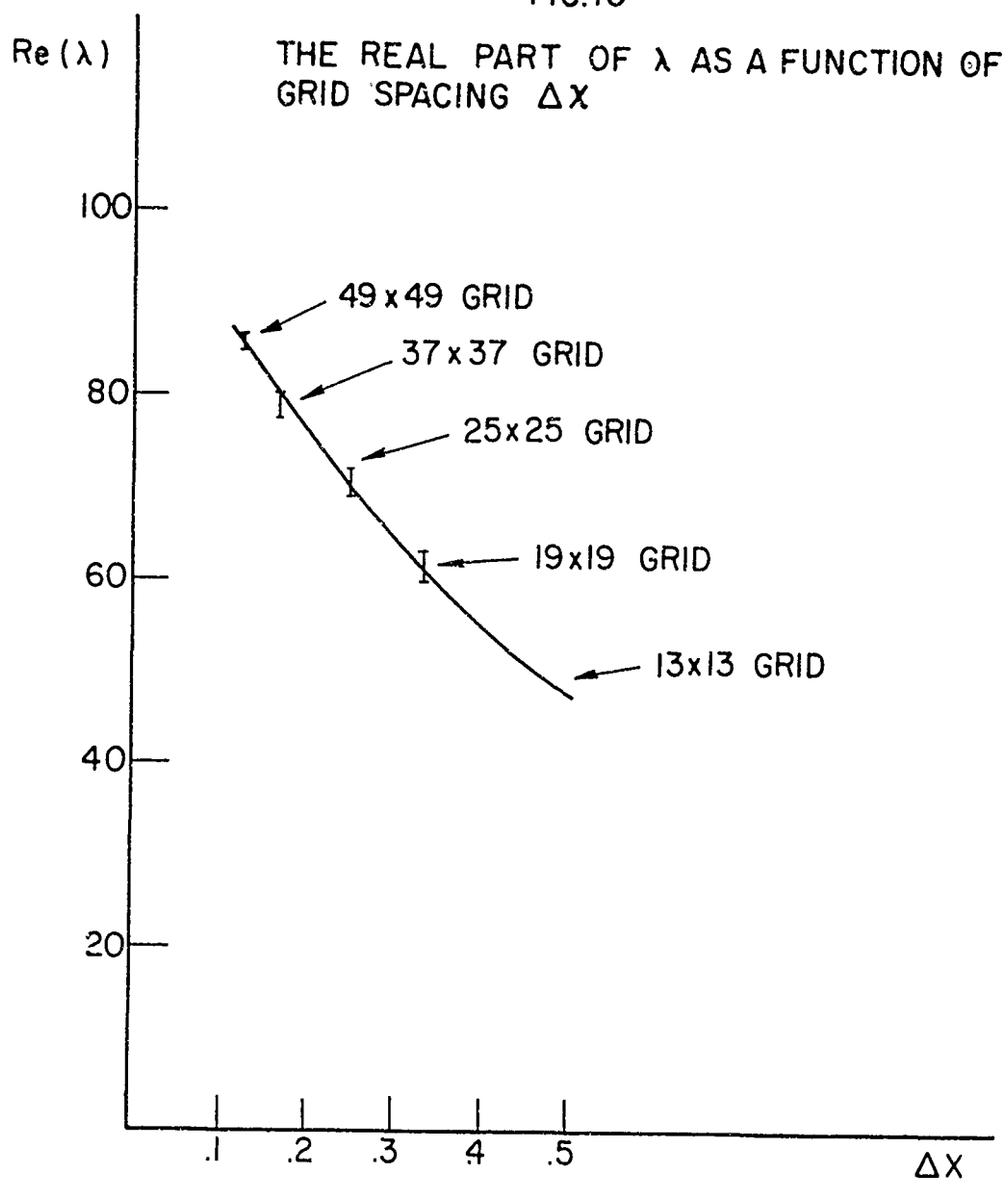

FIG. 11

LOG (ΔX) AS A FUNCTION OF THE REAL PART OF λ

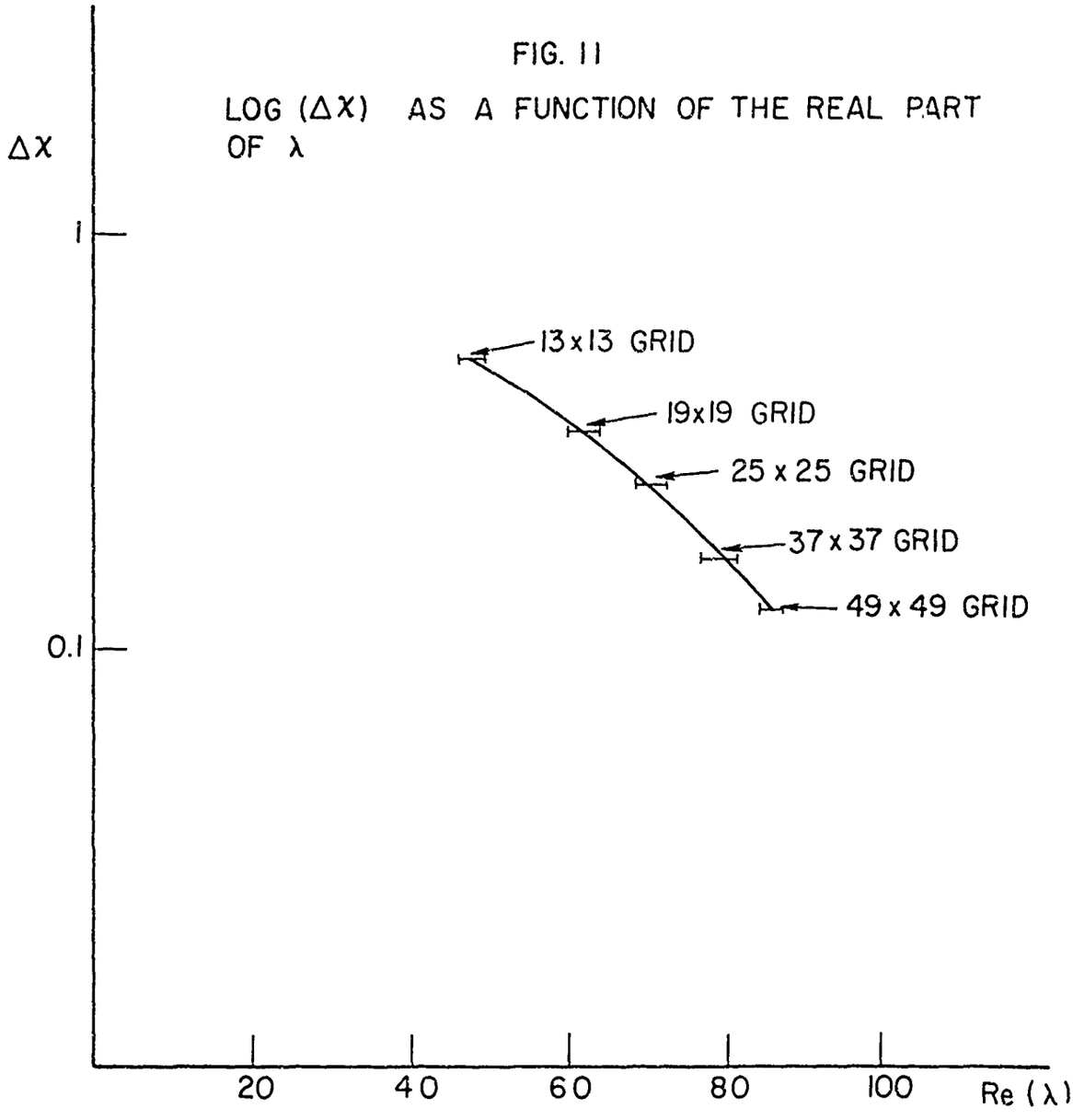

TABLE 1

List of Eigenvalues ($=\omega t$) versus Grid Size

Grid Size	Grid Spacing (Δx)	Eigenvalue
13x13	1/2	47.5±6.4i
19x19	1/3	61.2±3.2i
25x25	1/4	71.2±4.9i
37x37	1/6	78.5±8i
49x49	1/8	85.8±12i

UNCLASSIFIED

Security Classification

DOCUMENT CONTROL DATA - R&D

(Security classification of title, body of abstract and indexing annotation must be entered when the overall report is classified)

1. ORIGINATING ACTIVITY (Corporate author)	2a. REPORT SECURITY CLASSIFICATION
University of Rochester River Campus Rochester, New York 14627	Unclassified
	2b GROUP

3. REPORT TITLE

POLARIZATION, STEEPENING AND STRIATION IN BARIUM CLOUDS

4. DESCRIPTIVE NOTES (Type of report and inclusive dates)

Semi-Annual Technical Report 15 March 1971-14 September 1971

5. AUTHOR(S) (Last name, first name, initial)

Albert Simon
Arthur M. Sleeper

6. REPORT DATE	7a. TOTAL NO. OF PAGES	7b. NO. OF REFS
SEPTEMBER 1971	36	6

8a. CONTRACT OR GRANT NO.	9a. ORIGINATOR'S REPORT NUMBER(S)
F30602-70-C-0001	
b. PROJECT NO. ARPA Order 1057	
c. Program Code Number 1E20	9b. OTHER REPORT NO(S) (Any other numbers that may be assigned this report)
d.	RADC-TR-71-292

10. AVAILABILITY/LIMITATION NOTICES

Approved for public release; distribution unlimited.

11. SUPPLEMENTARY NOTES	12. SPONSORING MILITARY ACTIVITY
Monitored by: LEONARD STRAUSS RADC/OCSE Griffiss AFB NY 13440	Advanced Research Projects Agency 1400 Wilson Blvd Arlington VA 22209

13. ABSTRACT

Numerical results are presented for the diffusive growth in time of a barium cloud in a highly (but not infinitely) conducting ionosphere. Polarization effects produce steepening of the backside and a thinning and indentation on the front side. A crude estimate of the time required for appreciable distortion is given.

Numerical results are also given for the linearized equations of motion about an ellipsoidal gaussian equilibrium distribution. A new numerical method yields the fastest growing eigenvalue and eigenfunction and has been pushed to 49 x 49 size grids covering the cloud. The resultant eigenfunctions (in the plane perpendicular to the B field) are concentrated in the rear of the cloud and are elongated parallel to the cloud drift velocity. Finally, it is shown that results already available in the original E x B instability paper can be used to obtain an estimate of the striation scale size and onset time.

DD FORM 1 JAN 64 1473

UNCLASSIFIED

14. KEY WORDS	LINK A		LINK B		LINK C	
	ROLE	WT	ROLE	WT	ROLE	WT
1. Striations 2. E x B Instability 3. Cross Field Instability 4. Gradient Drift Instability 5. Barium Clouds 6. Steepening of Backside						

INSTRUCTIONS

1. ORIGINATING ACTIVITY: Enter the name and address of the contractor, subcontractor, grantee, Department of Defense activity or other organization *(corporate author)* issuing the report.

2*a*. REPORT SECURITY CLASSIFICATION: Enter the overall security classification of the report. Indicate whether "Restricted Data" is included. Marking is to be in accordance with appropriate security regulations.

2*b*. GROUP: Automatic downgrading is specified in DoD Directive 5200.10 and Armed Forces Industrial Manual. Enter the group number. Also, when applicable, show that optional markings have been used for Group 3 and Group 4 as authorized.

3. REPORT TITLE: Enter the complete report title in all capital letters. Titles in all cases should be unclassified. If a meaningful title cannot be selected without classification, show title classification in all capitals in parenthesis immediately following the title.

4. DESCRIPTIVE NOTES: If appropriate, enter the type of report, e.g., interim, progress, summary, annual, or final. Give the inclusive dates when a specific reporting period is covered.

5. AUTHOR(S): Enter the name(s) of author(s) as shown on or in the report. Enter last name, first name, middle initial. If military, show rank and branch of service. The name of the principal author is an absolute minimum requirement.

6. REPORT DATE: Enter the date of the report as day, month, year; or month, year. If more than one date appears on the report, use date of publication.

7*a*. TOTAL NUMBER OF PAGES: The total page count should follow normal pagination procedures, i.e., enter the number of pages containing information.

7*b*. NUMBER OF REFERENCES: Enter the total number of references cited in the report.

8*a*. CONTRACT OR GRANT NUMBER: If appropriate, enter the applicable number of the contract or grant under which the report was written.

8*b*, 8*c*, & 8*d*. PROJECT NUMBER: Enter the appropriate military department identification, such as project number, subproject number, system numbers, task number, etc.

9*a*. ORIGINATOR'S REPORT NUMBER(S): Enter the official report number by which the document will be identified and controlled by the originating activity. This number must be unique to this report.

9*b*. OTHER REPORT NUMBER(S): If the report has been assigned any other report numbers *(either by the originator or by the sponsor)*, also enter this number(s).

10. AVAILABILITY/LIMITATION NOTICES: Enter any limitations on further dissemination of the report, other than those imposed by security classification, using standard statements such as:

(1) "Qualified requesters may obtain copies of this report from DDC."

(2) "Foreign announcement and dissemination of this report by DDC is not authorized."

(3) "U. S. Government agencies may obtain copies of this report directly from DDC. Other qualified DDC users shall request through

_____."

(4) "U. S. military agencies may obtain copies of this report directly from DDC. Other qualified users shall request through

_____."

(5) "All distribution of this report is controlled. Qualified DDC users shall request through

_____."

If the report has been furnished to the Office of Technical Services, Department of Commerce, for sale to the public, indicate this fact and enter the price, if known.

11. SUPPLEMENTARY NOTES: Use for additional explanatory notes.

12. SPONSORING MILITARY ACTIVITY: Enter the name of the departmental project office or laboratory sponsoring *(paying for)* the research and development. Include address.

13. ABSTRACT: Enter an abstract giving a brief and factual summary of the document indicative of the report, even though it may also appear elsewhere in the body of the technical report. If additional space is required, a continuation sheet shall be attached.

It is highly desirable that the abstract of classified reports be unclassified. Each paragraph of the abstract shall end with an indication of the military security classification of the information in the paragraph, represented as *(TS)*, *(S)*, *(C)*, or *(U)*.

There is no limitation on the length of the abstract. However, the suggested length is from 150 to 225 words.

14. KEY WORDS: Key words are technically meaningful terms or short phrases that characterize a report and may be used as index entries for cataloging the report. Key words must be selected so that no security classification is required. Identifiers, such as equipment model designation, trade name, military project code name, geographic location, may be used as key words but will be followed by an indication of technical context. The assignment of links, rules, and weights is optional.

GPO 886-551